

3D Phase-shift Laser Scanning of Log Shape

Pedro Ah Shenga,* Peter Bomark, Olof Broman, and Olle Hagman

In this paper, a portable scanner to determine the 3D shape of logs was evaluated and compared with the measurement result of a computer tomography scanner. Focus was on the accuracy of the shape geometry representation. The objective is to find a feasible method to use for future data collection in Mozambique in order to build up a database of logs of tropical species for sawing simulations. The method chosen here was a 3D phase-shift laser scanner. Two logs, a birch log with bark, and a Scots pine log without bark were scanned, resulting in 450 cross sectional “images” of the pine log and 300 of the birch log. The areas of each point cloud cross section were calculated and compared to that of the corresponding computer tomography cross section. The average area difference between the two methods was 2.23% and 3.73%, with standard deviations of 1.54 and 0.91, for the Scots pine and birch logs, respectively. The differences in results between the two logs are discussed and had mainly to do with presence of bark and mantle surface evenness. Results show that the shape measurements derived from these methods were well correlated, which indicates the applicability of a 3D phase-shift laser scanning technology for gathering log data.

Keywords: Outer shape; Log measurement; 3D scanner; CT scanner

Contact information: Luleå University of Technology, Skellefteå Campus, SE-931 87, Skellefteå, Sweden;

**Corresponding author:* pedro.shenga@ltu.se

INTRODUCTION

Various methods are being used around the world to determine log shape to help sawyers optimize the value and volume yield of logs. The yield of processed softwood lumber can be improved with knowledge of the outer shape and inner features of logs prior to sawing (Grace 1993; Oja *et al.* 1998). Knowledge about the effect of such measurements and controls applied to tropical hardwood sawmills processes is incomplete. This is especially true for small hardwood sawmills in developing countries. The methods and techniques used are suitable for large sawmills, almost all of which require longitudinal conveyor transport of logs. This requirement is seldom satisfied at sawmills in developing countries. As a consequence, research about optimization potential and log positioning in small scale hardwood sawmills is hard to find. The vision of our future research is to study the impact of sawing patterns and log positioning, applying the best opening face (BOF) to study the value and volume yield of some tropical species and products in Mozambique. If future research show that Mozambican sawmills would benefit by using log shape measurement prior sawing, it may give incentives for small sawmills to invest in log scanning techniques. A brief description of the Mozambican wood processing industry follows.

The potential to improve the sawmill industry is great, as around 80% of logs are exported to Asian countries. The most common species exported are Umbila

(*Pterocarpus angolensis* D. C.), Jambirre (*Millettia stuhlmannii* Taub.), and Chanfuta (*Azelia quanzensis* Welw.) (Shenga *et al.* 2013). Today, requirements of exported sawn products are low because the market price of processed wood is lower than that of round wood in these markets (Ekman *et al.* 2013). The cause of this peculiar situation is twofold: First, Mozambican forest law does not allow export of round wood (some species are exempt from this). Second, the link between Mozambique and the export markets is made by Asian companies, whose preference is round wood for their domestic wood processing industries. As a consequence, most of the wood is exported as blocks to fulfill the minimum requirements of Mozambican forest laws.

Unfortunately, the current export situation gives sawmills few incentives for investment in further processing capabilities. Finding complementing or new markets or decreasing the use of intermediaries (hence doing business directly with their markets) could improve the current export market situation. If actions to improve the market integration are made, it can be assumed that requirements of wood products will rise, as will requirements of the wood processing operations. In such a situation, Mozambican sawmills must be capable of producing and offering products with changed or stricter quality requirements. A second assumption is that the Mozambican wood raw material itself, coming from dense and high-valued species, could if correctly handled, processed, and marketed, be sold and exported as high-quality lumber that meets the specifications of any market.

Mozambican sawmills are characterized by simple equipment. Often, a band headrig with low production capacity and a low level of automation is used. The high-density logs that are processed are fairly short (2 to 3 meters) but of large diameters and irregular outer shapes. Skilled sawyers are rare, and the salary for a sawyer is often low. The employees at sawmills are often self-taught with no formal education regarding the tasks of their work. Ad hoc solutions are often used, resulting in great waste and low efficiency in the use of raw materials. Knowledge of how to apply different breakdown strategies to reach high value and volume yield of the sawn products is, overall, lacking.

To increase Mozambican knowledge of how to process tropical species in an efficient way, significant research is required. The strategy of our future research will be to scan logs in Mozambique prior to sawing, store the empirical data in a database, and execute simulations and test different production strategies. This setup will make it possible to saw the “virtual” logs an unlimited amount of times in a saw simulator. The alternative is to do a large amount of exhaustive empirical test sawings. To accomplish this, we need a methodology to determine the outer shape of logs prior to sawing which is portable and suitable for the low tech situation at Mozambican sawmills. The equipment must be lightweight, easy to use, and suitable for outdoor scanning. A practical limitation is that the log must be still during scanning because no (or very few) Mozambican sawmills are equipped for conveyor transport of logs suitable for traditional scanning techniques.

Different techniques for the measurement of log shape and processing of the corresponding data exist. Keane (2007) describes a software AutoStem™, which imports data from a laser scanner and processes it automatically for each scan in about 3 to 5 min. The result can be exported to different saw optimization software packages with an outer shape description of every decimetre. Bhandarkar *et al.* (1999) investigated a system for the detection and rendering of internal log defects using computer tomography (CT). Antikainen and Verkasalo (2013) described the acquisition of log shape using structured light analysis in which the 3D modeling and calculations were performed with a

developed graphics processing unit. Pinto *et al.* (2003) used a WoodCim® inspector scanning system for the reconstruction of Maritime pine logs when sawing. All methods mentioned above require controlled, horizontal transport and/or rotation of logs during scanning, a requirement that can be problematic under typical Mozambican conditions.

Within the realm of portable scanners for potential use in structural geometric measurements of stationary objects, three primary ranging technologies are being used in the area of commercial laser scanners: (1) Time-of-flight discrete-return scanners; (2) Continuous wave phase-shift scanners; and (3) Time-of-flight waveform scanners. Time-of-flight discrete-return scanners pulse laser energy and measure the discrete time-of-flight of a return echo. They provide high accuracy even at large range (effective range is kilometers). The pulse frequency is usually around 100 thousand points per second. Phase based scanners emit a constant wave laser with its intensity modulated at a number of frequencies. They measure shifts in phase of the returned modulations to determine range. The phase based scanners can sample at much higher frequencies than time-of-flight scanners, around 1 million points per second, effective range is less than 100 meters. A phase based scanner is usually cheaper and lighter than a similar time-of-flight scanner. Time-of-flight waveform scanners record the full time trace of energy that is returned after a laser pulse has been emitted from the instrument. The key difference is that in the case of full waveform instruments, the full intensity trace is recorded for future analysis (Newnham *et al.* 2012). Terrestrial laser scanners (TLS) have been used for stand measurement and shape reconstruction (Simonse *et al.* 2003; Thies *et al.* 2004; Watt and Donoghue 2005; Maas *et al.* 2008; Dassot *et al.* 2012; Hilderbrant and Iost 2012; Kelbe *et al.* 2013).

However, TLS methods have some drawbacks if compared to the methods used to measure log shape in saw line. They require more than one scan position to get a full description of the object, which result in low acquisition speed. Moreover, the registration of scans is time-consuming and not automated enough requiring manual operations. Despite these disadvantages, TLS was found suitable for data collection for Mozambican sawmill environment. The phase-shift scanner was chosen for this study due to its benefits compared to Time-of-flight scanners.

Working principle for 3D phase-shift laser scanners

A sinusoidal, modulated laser beam is emitted and its reflection from an object is analyzed in order to determine the phase shift. The phase difference is proportional to the time taken by the laser to go to and from the object, and this time is proportional to the distance travelled. Laser technology is highly effective because the light wave is reflected from all solid surfaces with limited divergence, regardless of the nature of the obstacle. Thus, if f is the modulation frequency and T_l the phase shift, the distance d can be calculated according to following formula:

$$d = c \cdot T_l / 4 \cdot \pi \cdot f \quad (1)$$

where c is the speed of light. The measurement result is a point cloud of measurement spots that can be used to construct 3D volumes.

Studies regarding the transformations of 3D volumes have been made using a variety of different algorithms. Thomas *et al.* (2006) investigated the detection of defects in hardwood using circles fit with a generalized M-estimation method. Hilderbrant and

Iost (2012) used a polygon method considering the azimuth angle position to calculate the volume of a stem from point cloud data collected by TLS. In the latter method, the coordinates are put in order and a medial line is traced through them. The increase of angle and the area of the cross section are calculated as the sum of the triangles formed by the points. Two examples of other methods used to determine cross sectional areas are the Pratt method and the Shadow area method. The Pratt method is based on direct least-squares analysis, which fits a line between the scattered points and gives the center coordinates and the radius of the cross section for area calculations (Pratt 1987). In the Shadow area method, or two axis shadow scanning principle, the cross section is simplified into four coordinates resulting in an oval representation, and its area is calculated as the area of an ellipse using the major and minor axes of the cross section (Green 1993). These methods were tested, and the first method yielded a conical or cylindrical shaped log (obtained using parametric plotting). It was affected by the distribution of points in the cloud, whereas the second gave more details of the outer shape. Unfortunately, diameter values were sensitive to the positioning of the log during scan when using the second scanning method.

Computer tomography (CT) scanner

A CT scanner consists of an X-ray tube and a detector (photographic film, semiconductor, or array) that rotates around the object being measured. When a high-energy beam generated by the X-ray tube passes through an object, measurements of the attenuation of the X-ray emission are generated and collected by a detector. These measurements allow for the generation of a two-dimensional image of a slice or section through a three-dimensional object. In wood, mass attenuation is approximately constant, which allows for reliable calculation of its density. Such density images can be used to calculate numerous qualities of a cross section such as its diameter, area, and others. Computer tomography has frequently been used for research on log features (Oja *et al.* 1998; Nordmark 2003; Rinnhofer *et al.* 2003; Skog and Oja 2009).

Objective

The aim of this study was to test the applicability and accuracy of a 3D phase-shift laser scanner for measurement of the outer shapes of logs. The evaluation was made by comparing the measurements from the 3D scanner with those from a CT (X-ray) scanner. This study was limited to only two logs, one without bark (straight) and one with bark (crooked and irregular outer shape). Focus was on the outer shape representation and not the absolute value of *e.g.* diameter, volume *etc.* Due to its small sample, this study should be seen as preliminary and indicative. The test results will guide us in the suitability of using the 3D phase-shift laser scanner for future data collection in Mozambique and possibilities to investigate the effects of BOF, breakdown strategies, and log positioning in Mozambican hardwood sawmills.

EXPERIMENTAL

Materials

A 3D phase-shift laser scanner, FARO Focus 3D S-120 (USA), was selected for testing. For the evaluation, two logs were used: a three metre birch log (*Betula pendula* Roth.) and a four and a half metre Scots pine log (*Pinus sylvestris* L.). To test the

behavior of the 3D laser scanner for different surfaces, the birch log was scanned with bark, while the Scots pine log was scanned without bark (industrially debarked). Both logs were also scanned with a CT scanner (SOMATOM AR. T, Siemens AG; Germany), and the results were compared.

Methods

For each centimetre of the log, a cross sectional image of the log was gathered using the CT scanner. The length of the logs defined the number of resulting cross sections (300 for the three metre birch log and 450 for the four and a half metre Scots pine log). The CT scanner was set to produce 16-bit grayscale images. The image size was 512 x 512 pixels for a window size of 400 x 400 square millimeters, corresponding to a voxel size of 0.781 x 0.781 x 10 cubic millimeters.

The logs were then scanned individually with the 3D scanner from three positions. Figure 1 illustrates one of the scanning positions. Three spherical reference points were placed around the logs to allow precise registration of the scans. The range of the scans in the horizontal and vertical directions was limited to avoid scanning the surroundings and to speed up the operation. The position of the scanner with relation to the log determined the range setup. Each scan lasted around 6 minutes and describes millions of points with XYZ coordinates and RGB values. The point cloud (PC) data was registered, and unwanted information was removed using the Faro scanner software (SCENE version 5.2). The logs were then aligned in the XYZ coordinate system using CloudCompare (version 2.5.4.1) and saved in ASCII format before being imported into Matlab (MathWorks, USA) for calculation of cross sectional areas and comparison analysis.

The data were processed separately for each profiling method (as shown in the flow chart in Fig. 2) and then compared. The calculation of cross sectional area was done in Matlab using a Polygon method (Hilderbrant and Iost 2012).



Fig. 1. Setup for data acquisition. (1) Reference points; (2) 3D phase-shift laser scanner; (3) Computer tomography scanner and (4) the Scots pine log.

A description of how the images from the CT scanner and the PC data from the 3D scanner were manipulated and analyzed is presented in Fig. 2.

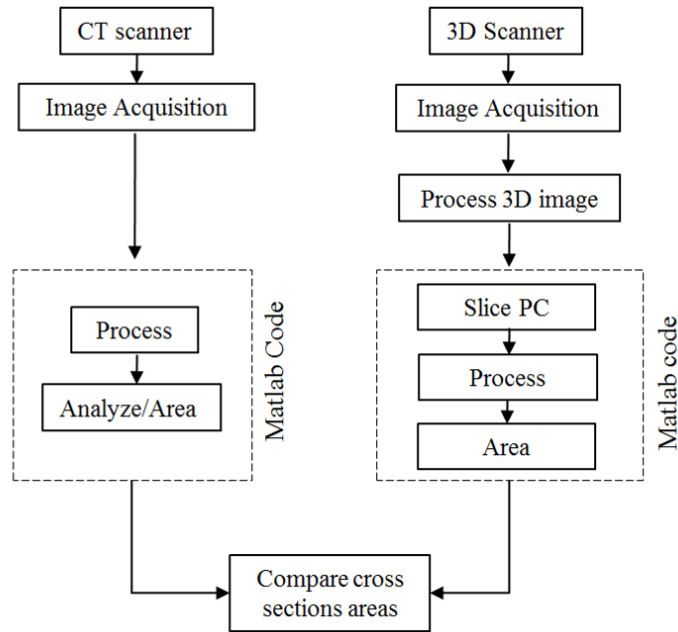


Fig. 2. Process flow chart of acquisition and processing for computer tomography (CT) and 3D scanner data.

CT data

The sequence of greyscale images, or cross sections, was loaded and processed for area determination as shown in Fig. 2 (left column). The results are shown in Fig. 3. The basic steps of data analysis were as follows: (1) The data (original data from CT scanner in .IMA format) was transformed to a file readable by Matlab. The result of this transformation is a file in a .tif format; (2) The transformed data was converted into an image (*mat2gray*), as shown in Fig. 3a; (3) A *median* filter (7 x 7) was applied, as shown in Fig. 3b; (4) Thresholding was applied to the filtered image resulting in a binary image, as shown in Fig. 3c. The threshold level was different for each cross section, with an average of 0.3; and (5) The cross sectional areas were determined, as shown in Fig. 3d, using the *regionprops* command. These values were saved in a worksheet.

PC data

The laser scans were registered with the help of the built in 3D phase-shift laser scanner software (SCENE), were aligned onto a XYZ coordinate system in CloudCompare 2.5.4.1, and were processed using a Matlab algorithm. Figure 2 (right column) shows a sequence of the process, and Fig. 4 shows an example of a cross section of point cloud data and its associated boundary description.

The point cloud data was first cropped to achieve the same log length as the CT data, and was sectioned in the same way as the CT cross sections (10 mm distance). The number and position of each cross section were tuned to be the same as in the CT case. The Matlab algorithm used is described as follows: (1) The data was loaded and color information was removed (the color information was not used in the test); (2) A size output was acquired by calculating the length of the log; (3) The distance between cross sections was set ($x = 10$ mm) and the number of cross sections was determined; (4) The points in Cartesian coordinates were converted to polar coordinates for each cross section and sorted according to increasing angle; (5) The area of each cross section was calculated using a polygon formula,

$$A = [(x_1 + x_2) \cdot (y_1 - y_2) + (x_2 + x_3) \cdot (y_2 - y_3) + \dots + (x_n + x_1) \cdot (y_n - y_1)] / 2 \quad (2)$$

where n is the number of vertices; and (6) The area values were saved in a worksheet file.

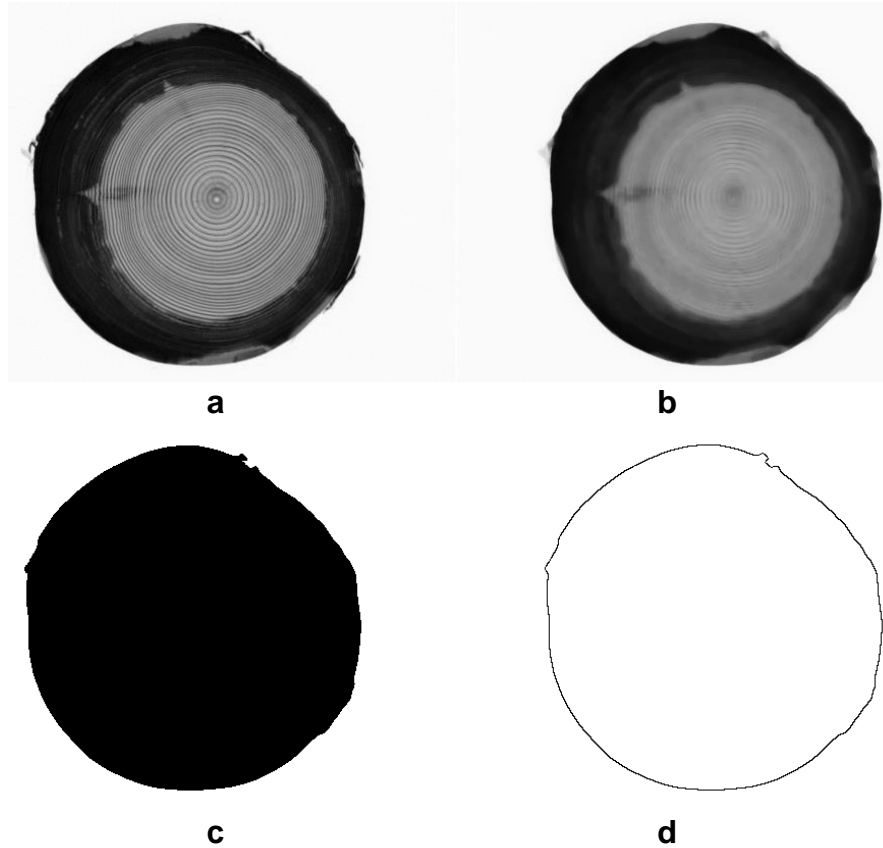


Fig. 3. Steps for determining the cross sectional area of CT images (Scots pine log): (a) original grayscale image; (b) filtered image; (c) threshold image; and (d) description of cross sectional boundary.

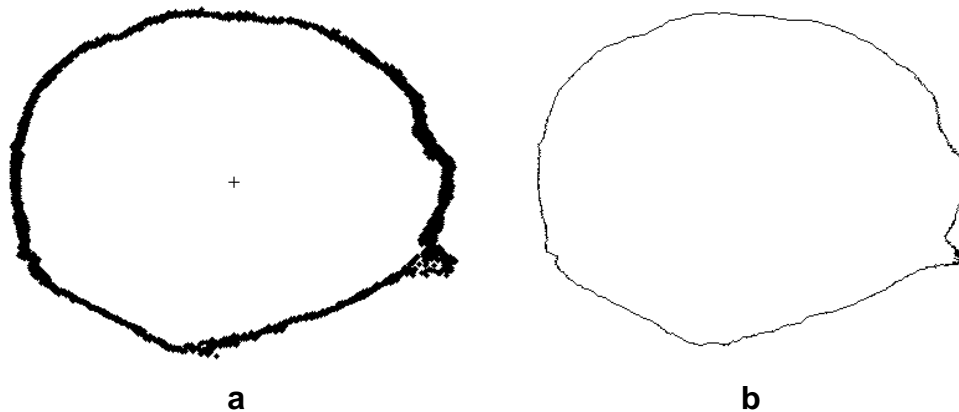


Fig. 4. Examples of cross sectional areas determined via 3D scanner data (birch log): (a) point cloud (PC) describing the boundary of the cross section; and (b) line fit to describe its boundary.

Finally, the cross sections of the CT slices and the corresponding cross sections from the 3D scanner were plotted in the same coordinate system for comparison. The average area difference and standard deviation were calculated.

RESULTS

Figures 5a and 6a show a longitudinal representation of the reconstructions of the two logs from point cloud (PC) data. In the 3D representation (which was difficult to show in manuscript format), external logs features were visible, such as the location of the butt and top ends, taper, and crook. Additionally, the surface mantle features were also visible; for instance, the presence of loose bark on the pine log and debranched knot marks and the presence of lichen on the birch log.

The 2D reconstruction of the Scots pine log, as shown in Fig. 5a, shows a white surface along the log, revealing incomplete data. This phenomenon was detected on the top and bottom of the log and could have been avoided by improved positioning of the 3D scanner. The lower left side of the log is also white but this is not missing data; rather, this was due to reflections of direct sunlight.

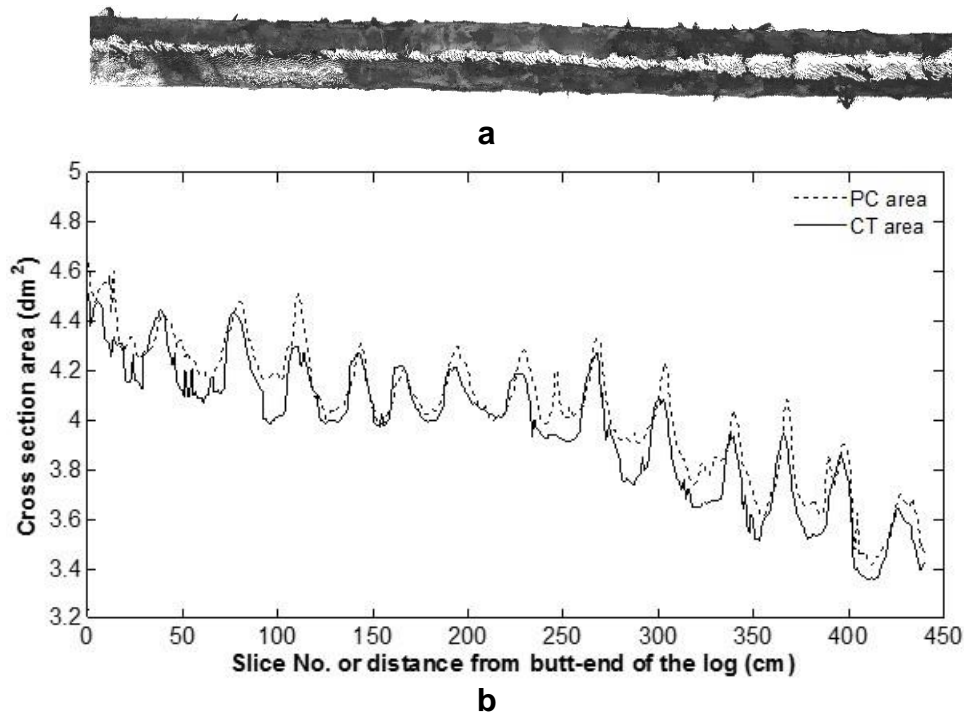


Fig. 5. (a) Reconstruction of point cloud data of the Scots pine log; and (b) comparison of cross sectional areas between data from the 3D scanner and computer tomography. The point cloud (PC) areas are represented with dotted line (- - -) and computer tomography (CT) areas with a continuous line (—).

For visual comparisons, the graphs in Figs. 5b and 6b show the cross sectional areas and their respective locations along the length of the logs. The CT areas were systematically smaller than the PC areas (note the offset between the solid and dotted line). This difference in area between the CT and PC scans was somewhat smaller for the

Scots pine logs than the birch log. The graphs also show the shape of the logs, the location of butt and top end, the taper, and the location of knot whorls.

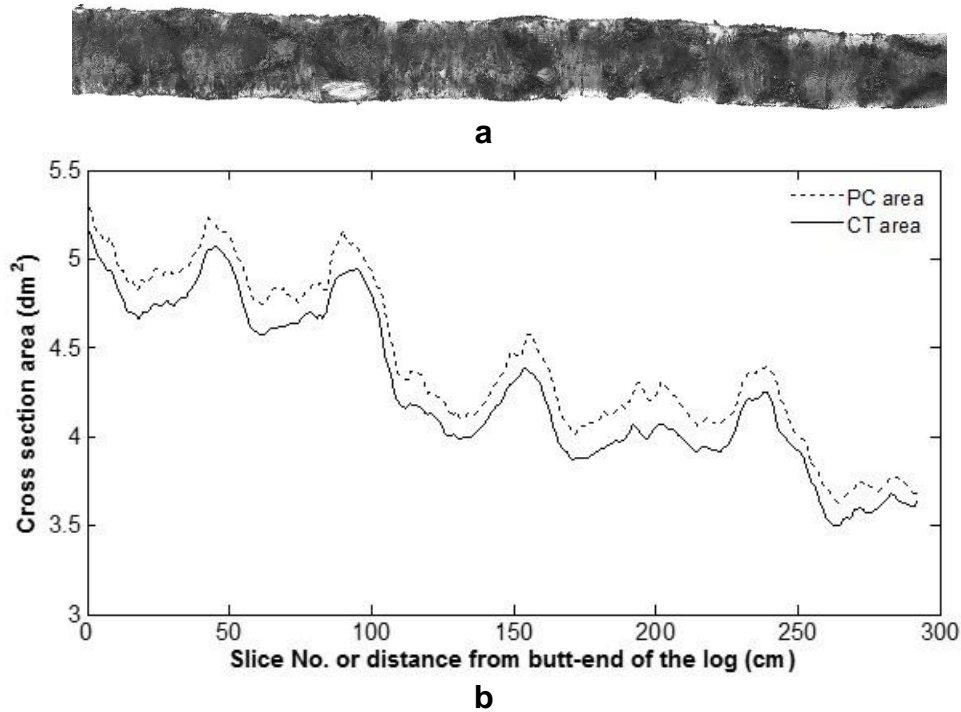


Fig. 6. (a) Reconstruction of point cloud data of the birch log; and (b) comparison of cross sectional areas between data from the 3D scanner and computer tomography. The point cloud (PC) areas are represented with dotted line (- - -) and computer tomography (CT) areas with a continuous line (-).

The average difference between the areas determined using the two methods was 2.23% and 3.73%, with standard deviations of 1.54 and 0.91, for the Scots pine and birch logs, respectively.

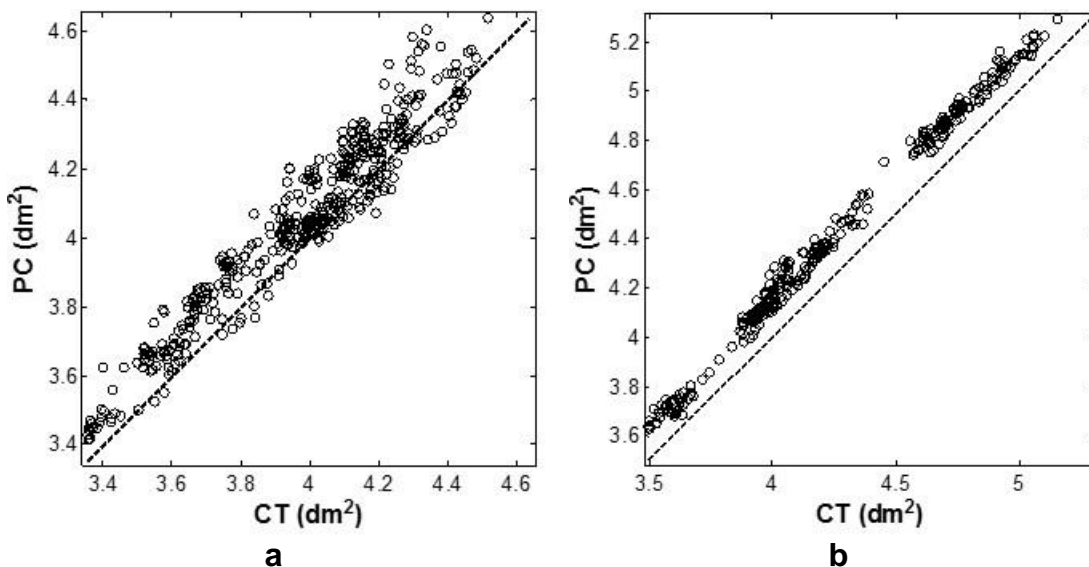


Fig. 7. (a) Scots pine data and (b) birch data. The plots shows that the CT and PC are correlated with $r = 0.962$ and $r = 0.997$ for pine and birch data, respectively

Despite the systematic difference between the results of the two methods, the measurements are correlated with $r = 0.962$ and $r = 0.997$ for pine and birch data, respectively. Figures 7a and 7b show the relation of data with an identity line. The systematic measurement error of the two logs is revealed by the closeness of points to the identity line. Pine data are more spread out but closer to the line, revealing higher standard deviation and smaller error between two methods, Fig. 7a. Whereas the small spread and the larger shift from the identity line of the birch data reveals lower standard deviation and bigger error, Fig. 7b.

DISCUSSION

Overall, the cross-sectional areas determined from point cloud (PC) data showed good agreement with the comprehensive computer tomography (CT) areas. However, some differences between the two methods were observed. There are some possible sources of error in the performed investigation including errors from the acquisition method itself, errors from the data processing method, and errors due to properties of the object scanned (log surface features like loose bark, scratches, cracks, and others). In Fig. 5b, some of these errors occasionally resulted in larger CT areas than PC areas. Furthermore, the same phenomenon is represented by values under the identity line, Fig. 7a. This may be a result of improper lengthwise matching of cross section positions caused by missing data at the butt and top ends of the logs (because of the device used to hold the logs during scan). The overlaps could be avoided by using fixed reference points on the log for both scan methods. Moreover, Fig. 8 shows an example of one cross section that was not fully described by the PC *i.e.*, representing missing data. The linear approximation that describes the PC boundary depends on the distribution of points along the scanned surface, meaning that irregularities on the surface of a log affect the point cloud measurement results.

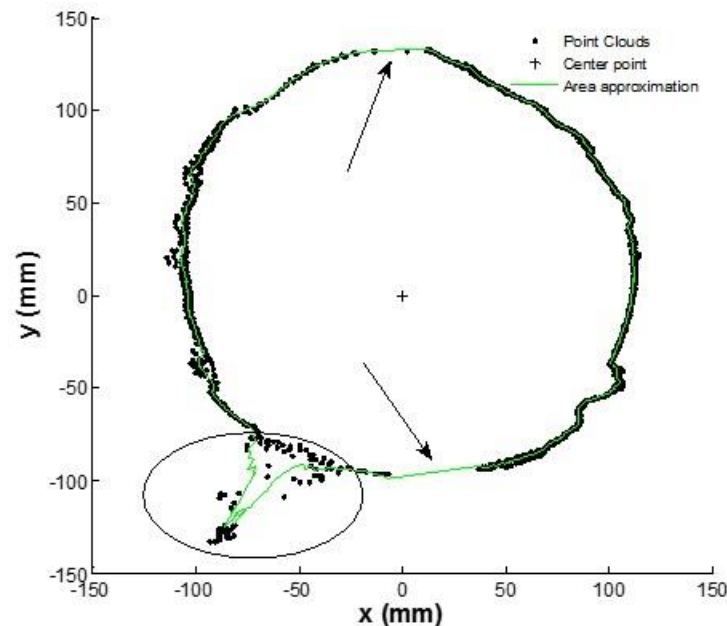


Fig. 8. Example of a Scots pine cross section from the point cloud data that shows missing data from the scanning indicated by arrows. The ellipse indicates an instance of loose bark being considered as part of the cross section.

Despite the absence of some data, the area estimation was not severely affected (Fig. 5b). Figure 8 also shows that loose bark was considered as part of the cross section, which of course affects the area estimations.

The somewhat more crooked birch log had few irregularities on the mantle surface, and the point cloud results agreed with properties of the real log as shown in Fig. 7b. The standard deviation value was low, only 0.91. The Scots pine log had many defects on the mantle surface such as cracks, scratches, and loose bark. Some of these defects increased the standard deviation and the data spread as shown in Fig. 7a. This spread reveals surface irregularities and was caused by industrial harvest, handling, and debarking.

The difference in area values seen in the birch plot, Fig. 6b, reveals a large systematic error, which might be caused by the presence of bark and lichen attached to the surface. This can be handled by subtraction when scanning logs with bark. Here, the average of the area difference can be used to remove the bark thickness mathematically if it is known. In practice, if the PC method should be used for diameter or volume estimation of logs, the systematic error shown here could be reduced by a calibration operation.

Differences in the cross sectional areas of the Scots pine and birch logs are in agreement with the results found in related works. Lerch *et al.* (2008) reported 2% inaccuracy when taking anthropometric measurements with a 3D body scanner and a CT scanner; Hildebrant and Iost (2012) reported a 1% difference when measuring a PVC (polyvinyl chloride) pipe stem model. Furthermore, previous studies made using a terrestrial laser scanner to measure stems provided results that agree with our findings. Dassot *et al.* (2012) reported accuracy to within 10% when estimating the volume of the stem of trees and to within 30% when estimating that of tree branches. Kelbe *et al.* (2013) reported an accuracy of 12.5% with a 4.5% overestimation when reconstructing 3D stem models using low-cost TLS.

One way to improve the PC data acquisition is to avoid point cloud outliers. This can be achieved by cleaning the logs mantle surfaces prior scanning or by using improved methods for data processing before the area calculation, for instance the method described by Thomas *et al.* (2004). Despite these deficiencies in data acquisition and that only two logs were measured, the study show that a 3D phase-shift laser can be used for log geometry measurement. With experience from this preliminary test we recommend this methodology to be tested on a larger sample of logs, compared with other existing scanners to clarify the accuracy in and suitability for log volume measurement.

CONCLUSIONS

1. The point cloud data provide a detailed description of a logs external geometry and shape and showed good compliance with the reference measurement made with computer tomography.
2. The impact of the systematic error incurred with point cloud measurement can be reduced or handled by calibration operations (not investigated here). The error can also be reduced by cleaning up the mantle surface prior scanning and thus avoiding outliers in the point cloud measurement.

3. The test results show that the 3D phase-shift laser scanner is feasible to use for our future data collection in Mozambique aiming at investigating effects of BOF, breakdown strategies, and log positioning in Mozambican hardwood sawmills.

REFERENCES CITED

- Antikainen, J., and Verkasalo, E. (2013). "A real-time 3D log modelling for sawing optimization in a small circular sawmill," *Proceedings of the 21st Wood Machining Seminar*, 4-7 August, Tsukuba, Japan, pp. 75-82.
- Bhandarkar, S. M., Faust, T. D., and Tang, M. (1999). "Catalog: A system for detection and rendering of internal log defects using computer tomography," *Machine Vision and Applications* 11(4), 171-190. DOI: 10.1007/s001380050100 171-190
- Dassot, M., Colin, A., Santenoise, P., Fournier, M., and Constant, T. (2012). "Terrestrial laser scanning for measuring the solid wood volume, including branches, of adult standing trees in the forest environment," *Computers and Electronics in Agriculture* 89, 86-93. DOI: 10.1016/j.compag.2012.08.005
- Grace, L. A. (1993). *Using Optical Log Scanners to Determine Log Properties: Initial Results from SCA's Munksund Sawmill*, Swedish University of Agricultural Sciences Department of Forest Products. Report No. 232.
- Green, J. (1993). "3-D Log scanning and optimization," *Proceedings of the Scanning Technology and Process Control for the Wood Industry (SCANPRO'93)*, Atlanta, GA.
- Hildebrandt, R., and Iost, A. (2012). "From points to numbers: A database-driven approach to convert terrestrial LiDAR point clouds to tree volumes," *European Journal of Forest* 131(6), 1857-1867. DOI: 10.1007/s10342-012-0638-1
- Keane, K. (2007). *The Potential of Terrestrial Laser Scanning Technology in Pre-Harvesting Timber Measurement Operations*, Harvesting/Transportation 7, Coford Connects, Coford, Dublin, Ireland.
- Kelbe, D., Romanczyk, P., Aardt, J. V., and Cawse-Nicholson, K. (2013). "Reconstruction of 3D tree stem models from low-cost terrestrial laser scanner data," *Proceedings of the Laser Radar Technology and Applications XVIII*, (8731), 20 May, Baltimore, Maryland, USA. DOI: 10.1117/12.2015963
- Lerch, T., Anthony, S., and Domina, T. (2008). "Initial validation of point cloud data from a 3D body scanner," *International Journal of Clothing Science and Technology* 20(5), 271-280.
- Maas, H. - G., Bienert, A., Scheller, S., and Keane, E. (2008). "Automatic forest inventory parameter determination from terrestrial laser scanner data," *International Journal of Remote Sensing*, 29(5), 1579-1593. DOI: 10.1080/01431160701736406
- Newnham, G., Armston, J., Muir, J., Goodwin, N., Tindall, D., Culvenor, D., Puschel, P., Nystrom, M., and Johansen, K. (2012). *Evaluation of Terrestrial Laser Scanners for Measuring Vegetation Structure*, CSIRO Sustainable Agriculture Flagship, Manuscript ID: EP124571.
- Nordmark, U. (2003). "Models of knots and log geometry of young *Pinus sylvestris* saw logs extracted from computed tomographic images," *Scandinavian Journal of Forest Research* 18(2), 168-175. DOI: 10.1080/02827580310003740

- Oja, J., Grundberg, S., and Grönlund, A. (1998). "Measuring the outer shape of *Pinus sylvestris* saw logs with an X-ray log scanner," *Scandinavian Journal of Forest Research* 13(1-4), 340-347. DOI: 10.1080/02827589809382993
- Pinto, I., Pereira, H., and Usenius, A. (2003). "Analysis of log shape and interval knots in twenty Maritime pine (*Pinus pinaster* Ait.) stems based on visual scanning and computer aided reconstruction," *Ann. For. Sci.* 60(2), 137-144. DOI: 10.1051/forest:2003006
- Pratt, V. (1987). "Direct least-squares fitting of algebraic surfaces," *Proceedings of the 14th Annual Conference on Computer Graphics and Interactive Techniques (SIGGRAPH '87)*, Maureen C. Stone (ed.), ACM, New York. DOI: 10.1145/37401.37420
- Rinnhofer, A., Petutschnigg, A., and Andreu, J. (2003). "Internal log scanning for optimizing breakdown," *Computers and Electronics in Agriculture*, 41(1-3), 7-21. DOI: 10.1016/S0168-1699(03)00039-5
- Shenga, P., Cristóvão, L., and Broman, O. (2013). "A review of Mozambican wood exploitation - Map of the processing chain," *Proceedings of the 21st Wood Machining Seminar*, 4-7 August, Tsukuba, Japan, pp. 293-301.
- Simonse, M., Aschoff, T., Spiecker, H., and Thies, M. (2003). "Automatic determination of forest inventory parameters using terrestrial lasers scanning," *Proceedings of the ScandLaser Scientific Workshop on Airborne Laser Scanning of Forests*, pp. 252-258.
- Skog, J., and Oja, J. (2009). "Heartwood diameter measurement in *Pinus sylvestris* sawlogs combining X-ray and three dimensional scanning," *Scandinavian Journal of Forest Research* 24(1), 182-188. DOI: 10.1080/02827580902806585
- Thies, M., Pfeifer, N., Winterhalder, D., and Gorte, B. G. H. (2004). "Three-dimensional reconstruction of stems for assessment of taper, sweep and lean based on laser scanning of standing trees," *Scandinavian Journal of Forest Research*, 19(6), 571-581, DOI: 10.1080/028275804110019562
- Thomas, L., Mili, L., Shuffer, C. A., and Thomas, E. (2004). "Defect detection on hardwood logs using high resolution three-dimensional laser scan data," *Proceedings of International Conference on Image Processing (ICIP)*, 243-246 (1). DOI: 10.1109/ICIP.2004.1418735
- Thomas, L., Mili, L., Thomas, E., and Shaffer, C. A. (2006). "Defect detection on hardwood logs using laser scanning," *Wood and Fiber Science* 38(4), 682-695.
- Watt, P. J., and Donoghue, D. N. M. (2005). "Measuring forest structure with terrestrial laser scanning," *International Journal of Remote Sensing*, 26(7), 1437-1446, DOI: 10.1080/01431160512331337961

Article submitted: August 13, 2014; Peer review completed: October 15, 2014; Revised version received and accepted: October 24, 2014; Published: October 29, 2014.